

# The Influence of Temperature and Cyclic Frequency on the Fatigue Fracture of Cube Oriented Nickel-Base Superalloy Single Crystals

G. R. LEVERANT AND M. GELL

Carbon-free single crystals of Mar-M200 were tested in pulsating tension, stress-controlled fatigue at temperatures ranging from 1033 to 1255°K and 0.033 to 1058 Hz, respectively. The axis of loading was parallel to [001], the natural growth direction for directionally-solidified nickel-base alloys. Except for the lowest frequency at the higher temperatures where creep damage was extensive, crack initiation occurred at sub-surface microporosity. Cracks initiated and propagated in the Stage I mode (crystallographic cracking on the {111} slip planes) at the lower temperatures and higher frequencies, whereas Stage II (perpendicular to the principal stress axis) crack initiation and propagation was found at the higher temperatures and lower frequencies. Often a transition from Stage II to Stage I crack propagation was observed. It was established that Stage I cracking occurred under conditions of heterogeneous, planar slip and Stage II cracking under conditions of homogeneous, wavy slip. A thermally activated recovery process with an activation energy of 368 KJ/mole (88 Kcal/mole) determined the instantaneous slip character, *i.e.*, wavy or planar, at the crack tip. In addition, it was found that an optimum frequency existed for maximizing fatigue life. At frequencies below the optimum, creep damage was detrimental, while at frequencies greater than the optimum, intense, planar slip was detrimental. The optimum frequency increased with increasing temperature.

PREVIOUS studies of the fatigue fracture<sup>1-3</sup> and monotonic deformation<sup>4,5</sup> behavior of columnar-grained and single-crystal Mar-M200 have indicated a relationship between temperature, strain rate, slip character, and fracture mode. This past work showed a tendency for low temperatures and high strain rates to favor planar, heterogeneous slip and crystallographic fatigue cracking along {111} slip planes (Stage I cracking); whereas, high temperatures and low strain rates led to wavy, homogeneous slip and fatigue fracture perpendicular to the principal stress axis (Stage II cracking).

These trends suggested that a systematic variation of temperature and cyclic frequency (strain rate) might lead to a further understanding and quantification of the interrelationship among slip character and transgranular fracture mode, *i.e.*, Stage I vs Stage II fatigue cracking. With that objective in mind, this study was undertaken.

## I. MATERIAL AND EXPERIMENTAL PROCEDURE

Low carbon single crystals of the superalloy Mar-M200 were tested in stress-controlled, pulsating tension fatigue in air at temperatures ranging from 1033 to 1255°K ( $\sim 0.6$  to  $0.77 T_M$ ) and frequencies ranging from 0.033 to 1058 Hz. The tensile axes of the crystals were within 5 deg of the [001] direction. The composition of the alloy, its microstructure and heat treat-

ment, and the specimen configuration have been published previously.<sup>6,7</sup> Testing at frequencies up to 20 Hz was performed on a closed-loop MTS servo-hydraulic machine, whereas the tests at higher frequencies were performed on a magnetostrictive fatigue unit. All specimens were cycled from a minimum stress of 34.4 MN/m<sup>2</sup> (5 ksi) to a maximum stress which varied with temperature (Table I).

Thin foils for transmission electron microscopy were prepared by established procedures and examined in a Phillips EM-200 electron microscope.

## II. EXPERIMENTAL RESULTS

### A. Fatigue Data

The fatigue data for the various temperatures and frequencies are summarized in Table I and Figs. 1 and 2. It is evident from Fig. 1 that an optimum frequency exists for maximizing the cycles to failure as had been previously observed for a wrought, polycrystalline nickel-base superalloy.<sup>8</sup> The optimum frequency increased with increasing temperature as indicated by the fact that the data at 1200 K (1700°F) exhibited no drop off at high frequencies, at least up to the maximum frequency tested, *i.e.*, 600 Hz. It would be expected that a drop off would be seen at higher frequencies at this temperature. Fig. 2, which is a plot of fatigue life on a time basis vs frequency, shows two distinct regimes. At low frequencies at 1116 and 1200 K (1550 and 1700°F) the time to failure is roughly constant, indicating that creep is playing an important role in controlling the fatigue behavior. However, at all frequencies at 1033 K (1400°F) and the higher frequencies at 1116 K, the data has a slope

G. R. LEVERANT and M. GELL are affiliated with the Materials Engineering and Research Laboratory, Pratt and Whitney Aircraft, Middletown and East Hartford, Conn.

Manuscript submitted May 20, 1974.

Table I. Fatigue Test Data and Fractographic Observations

Specimen	Stress Range (MN/m <sup>2</sup> )	Elastic Strain Range (pct)	Frequency (Hz)	Cycles to Failure	Time to Failure (H)	Fractographic Observations
<b>1033 K (1400°F)</b>						
A4M3R	34.4-551*	0.5	0.75	4.18 × 10 <sup>5</sup>	155	Subsurface initiation at micropore-crack initiation on two Stage I facets and one Stage II facet.
A4M2R	34.4-551	0.5	0.75	2.69 × 10 <sup>5</sup>	99.7	Subsurface initiation at micropore-crack initiation on single Stage I facet.
A4M2L	34.4-551	0.5	2	3.95 × 10 <sup>5</sup>	55	Subsurface initiation at micropore-crack initiation on three Stage I facets and one Stage II facet.
A4M3L	34.4-551	0.5	2	4.57 × 10 <sup>5</sup>	63.5	Subsurface initiation at micropore-crack initiation on single Stage I facet.
X4J1	34.4-551	0.5	10	4 × 10 <sup>5</sup>	11.1	Subsurface initiation at micropore-crack initiation on single Stage I facet.
Z4J2L	34.4-551	0.5	1058	6 × 10 <sup>4</sup>	1.58 × 10 <sup>-2</sup>	Subsurface initiation at micropore-crack initiation on single Stage I facet.
Z4J3L	34.4-620	0.57	1058	6.77 × 10 <sup>4</sup>	1.78 × 10 <sup>-2</sup>	Subsurface initiation at micropore-crack initiation on single Stage I facet.
<b>1116 K (1550°F)</b>						
A4MIR	34.4-551	0.54	0.033	6.44 × 10 <sup>3</sup>	54.3	Surface initiation at multiple Stage II facets.
A4M1L	34.4-551	0.54	0.5	6.98 × 10 <sup>4</sup>	38.8	Subsurface initiation at micropore-crack initiation on single, circular Stage II facet. Transition to Stage I before failure.
X4W2	34.4-551	0.54	5.0	5.72 × 10 <sup>5</sup>	31.8	Subsurface initiation at micropore-crack initiation on single, circular Stage II facet. Transition to Stage I before failure.
Z4G2	34.4-551	0.54	20	2.59 × 10 <sup>5</sup>	3.6	Subsurface initiation at micropore-crack initiation on one Stage I and one Stage II facet.
A4P2L	34.4-551	0.54	1030	1.05 × 10 <sup>5</sup>	2.83 × 10 <sup>-2</sup>	Subsurface initiation at micropore-crack initiation on three Stage I facets.
Z4J2R	34.4-551	0.54	1030	1.03 × 10 <sup>5</sup>	2.67 × 10 <sup>-2</sup>	Subsurface initiation at micropore-crack initiation on three Stage I facets.
<b>1200 K (1700°F)</b>						
Z4GR	34.4-448	0.48	0.033	6.17 × 10 <sup>2</sup>	5.2	Surface initiation at multiple Stage II facets.
X4J7	34.4-448	0.48	10	9.5 × 10 <sup>4</sup>	2.64	Subsurface initiation at micropore-crack initiation on single, circular Stage II facet. Transition to Stage I before failure.
X4I5	34.4-448	0.48	10	4.3 × 10 <sup>5</sup>	11.9	Subsurface initiation at micropore-crack initiation on single, circular Stage II facet. Transition to Stage I before failure.
X5M3	34.4-448	0.48	600	1.2 × 10 <sup>6</sup>	0.56	Subsurface initiation at micropore-crack initiation on Stage I and Stage II facets.
<b>1255 K (1800°F)</b>						
X5L1	34.4-344	0.39	10	1.63 × 10 <sup>5</sup>	4.52	Subsurface initiation at micropore-crack initiation on single, circular Stage II facet. No transition to Stage I before failure.

\*ksi X 6.89 = MN/m<sup>2</sup>.

of nearly -1 (actually -1.3), indicating that fatigue in this regime is strictly cycle dependent.

### B. Fractography

With the exception of the tests run at a frequency of 0.033 Hz at 1116 and 1200 K where creep was extensive, all fatigue initiation sites occurred at subsurface microporosity (~0.1 mm in size). The reason for the subsurface initiation sites at the lower temperatures is the difficulty in initiating surface cracks due to slip dispersal caused by surface oxidation of slip steps and at the higher temperatures the difficulty in propagating surface cracks due to oxidation of the crack tip and the crack faces. These effects have been discussed in detail elsewhere<sup>1,9</sup> and will not be discussed further here.

It was found, as summarized in Table I, that Stage I crack initiation was favored at the lower temperatures and higher frequencies and Stage II crack initiation at the higher temperatures and lower frequencies. Figs. 3(a) and (b) show the fracture surfaces developed at frequencies of 5 and 1030 Hz at 1116 K, respectively. At 5 Hz, Stage II crack initiation occurred at the location indicated by the arrow and propagated radially until a transition to Stage I crystallographic cracking occurred at the periphery of the circular area. The symbols "A" are located on the Stage I facet. At 1030 Hz, however, crack initiation (arrow) and propagation occurred entirely in the Stage I mode. (X-ray analysis has shown these Stage

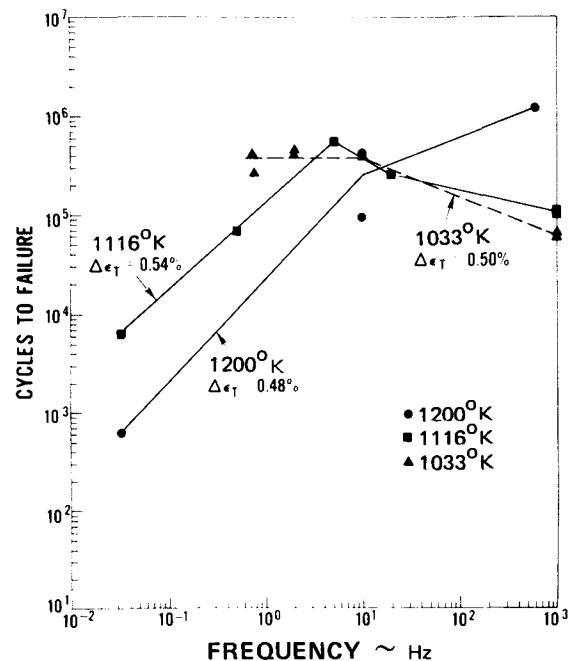


Fig. 1—The influence of cyclic frequency on the cycles to failure for Mar-M200 single crystals tested at 1033, 1116, and 1200 K.

I facets to be the {111} slip planes, which is in agreement with previous observations after room temperature fatigue testing.<sup>1,2</sup>) At a given frequency or frequency range at each temperature, Table I, both Stage

I and Stage II cracks were found emanating from the same micropore. The cyclic frequency at which this occurred increased from 0.75 to 2 Hz at 1033 K to 600 Hz at 1200 K.

The amount of fracture surface formed by either Stage I or Stage II crack propagation is shown in Fig. 4 as a function of temperature and frequency. The percentage of Stage I crack propagation increased with increasing frequency and decreasing temperature, where Stage II crack propagation occurred in greater percentages at high temperatures and low frequencies. For example, at 1116 K the percentage of Stage I crack propagation increased from zero to 100 pct by increasing the cyclic frequency from 0.033 to 1030 Hz. Likewise, at 10 Hz, the percentage of Stage I crack propagation increased from zero to 100 pct by decreasing the temperature from 1255 to 1033 K.

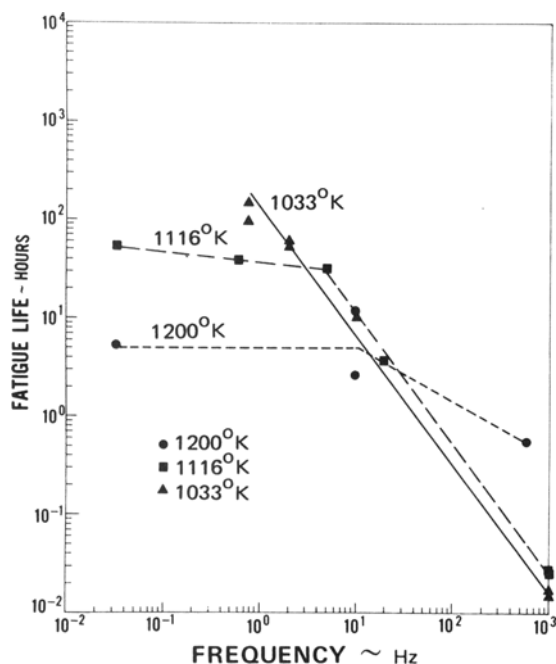
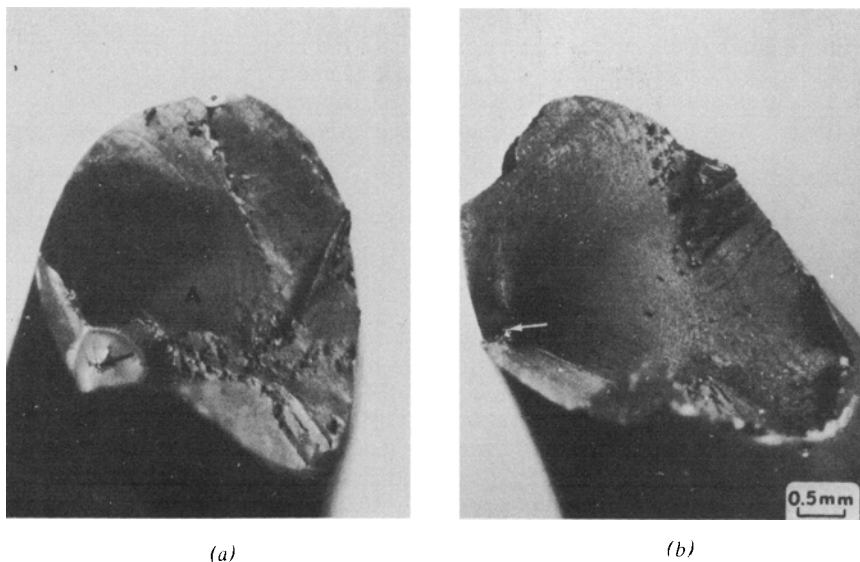


Fig. 2—The influence of cyclic frequency on the time to failure for Mar-M200 single crystals tested at 1033, 1116, and 1200 K.

Fig. 3—Optical fractographs of specimens tested to failure at 1116°K at frequencies of (a) 5 Hz and (b) 1030 Hz.



### C. Substructural Observations

Transmission micrographs of the dislocation substructure developed at frequencies of 0.033, 20, and 1030 Hz at 1116 F are shown in Figs. 5(a), (b), and (c), respectively. At the lowest frequency, the substructure was homogeneous and the density of dislocations was high because of the extensive creep encountered. At 20 Hz, the substructure was still homogeneous, but the dislocation density was considerably reduced because of the lower amount of creep strain. At the highest frequency, the dislocation density was extremely low and the dislocations were distributed heterogeneously in what appeared to be planar bands which had relaxed and recovered upon unloading and cooling to room temperature.

These observations, together with earlier work,<sup>1,5</sup> show that a correlation exists between the cracking modes and the deformation modes. At high frequencies and low temperatures, deformation in heterogeneously distributed planar bands leads to Stage I fatigue crack initiation and propagation. On the other hand, Stage II crack initiation and propagation are enhanced by homogeneously distributed slip which is developed at low frequencies and high temperatures.

## III. DISCUSSION

### A. Criteria for the Formation of Stage I and Stage II Fatigue Cracks at Temperatures $> 0.5 T_M$

Since the experimental observations show that Stage I cracking is dominant at high frequencies and low temperatures and Stage II cracking at low frequencies and high temperatures, one can deduce that thermally activated deformation processes must be involved in determining the fatigue fracture mode. It is likely, for example, that planar bands of dislocations are generated at the tip of stress concentrations such as micropores or existing cracks at most frequencies, but the planar bands are unstable with respect to thermally activated recovery processes such as dislocation climb or cross slip.

The presence of planar bands of dislocations is required to develop Stage I cracks; however, the crack

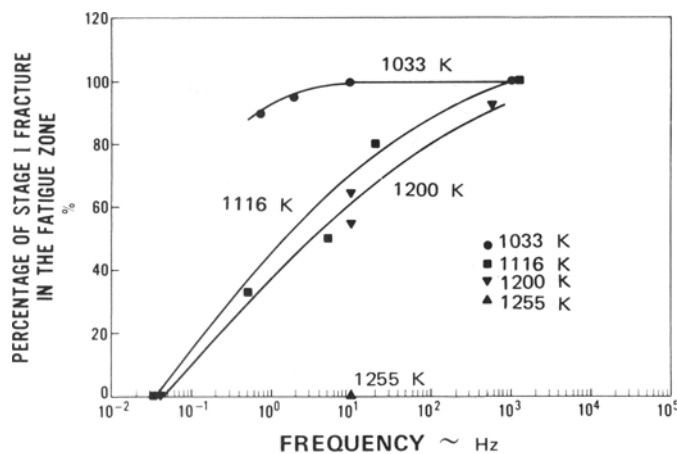


Fig. 4—The percentage of Stage I fracture in the fatigue zone as a function of cyclic frequency at temperatures of 1033, 1116, 1200, and 1255 K.

must form along the slip band at a rate which exceeds the rate of dislocation recovery out of the bands. Schematically, this is shown in Fig. 6 for the case where a Stage II crack is just about to advance for the various indicated conditions. At high frequencies or low temperatures, the planar bands have not dispersed and a Stage I crack can form along them. At high temperatures or low frequencies, the rate of dispersal of the dislocations in the planar bands exceeds the rate of crack formation along the bands and Stage II cracking would be expected. For intermediate conditions, either Stage I or Stage II cracks can form.

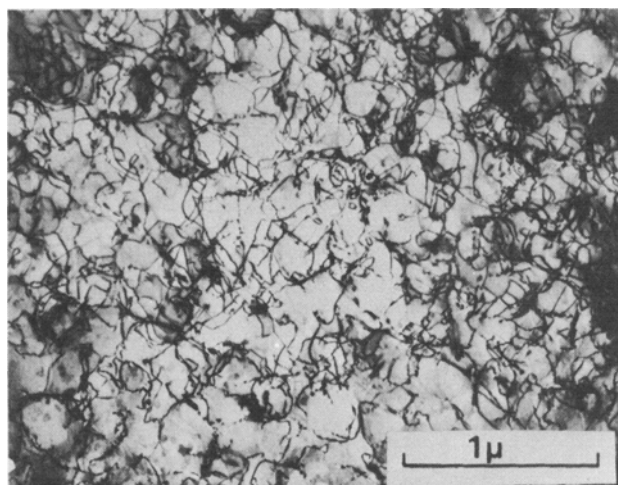
The conditions at which both Stage I and Stage II cracks initiate from the same micropore are considered to be those where the rate of dispersal of dislocations out of the planar bands is just equal to the rate of formation of Stage I cracks. Consequently, the frequency at which this occurs should increase with increasing temperature according to Arrhenius rate kinetics, *i.e.*, rate  $\sim \bar{v} \exp(-\Delta H/RT)$ . In fact, this critical frequency was found to be 0.75-2, 20, and 600 Hz at 1033, 1116, and 1200 K, respectively. A plot of the logarithm of this critical frequency (converted to strain rate) *vs* the inverse of the absolute temperature is a straight line, Fig. 7. The activation energy obtained from the slope of this line is 368 KJ/mole (88 Kcal/mole). This value is comparable to the values obtained for creep of Ni-Cr solid solutions<sup>10</sup> as well as single phase  $\gamma'$ ,<sup>11</sup> where diffusion-controlled climb should be rate controlling. Therefore, it is likely that dislocation climb out of planar bands at the crack tip is the critical thermally activated process determining whether Stage I or Stage II fatigue cracking occurs.

### B. Influence of Frequency on Fatigue Lives

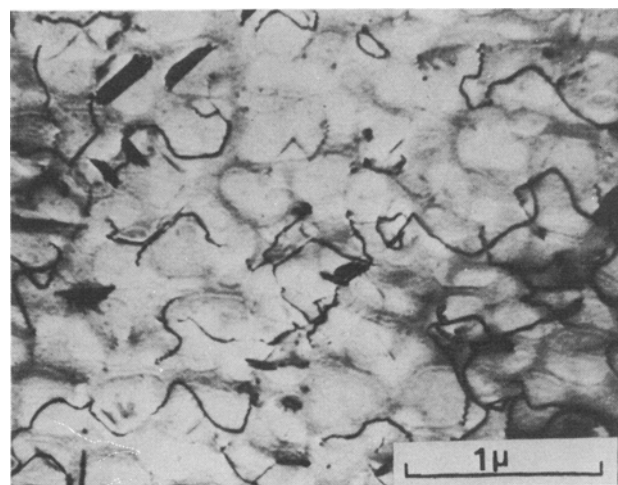
The fatigue lives at 1116 and 1200 K are quite low at the lowest frequencies. This is caused by extensive specimen creep during testing and, at 0.033 Hz, leads to surface initiated Stage II cracking. These are the only cases of surface-initiated cracking leading to failure in this study and can be attributed to large local plastic strains caused by creep. At 1033 K for the frequencies tested, creep was never a factor as indicated by the absence of a drop off at the lowest

frequencies and the absence of a break in the time to failure *vs* frequency plot, Fig. 2.

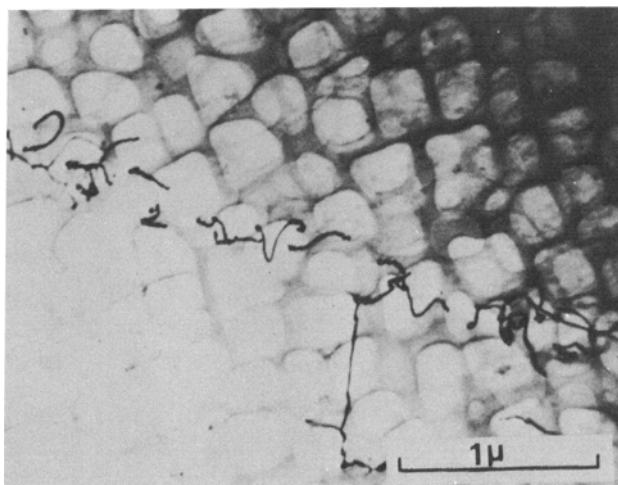
As the frequency increased, creep was suppressed, Figs. 5(a) and (b), and the fatigue lives increased as



(a)



(b)



(c)

Fig. 5—Transmission electron micrographs of the dislocation substructure in crystals tested at 1116 K at frequencies of (a) 0.033 Hz, (b) 20 Hz, and (c) 1030 Hz.

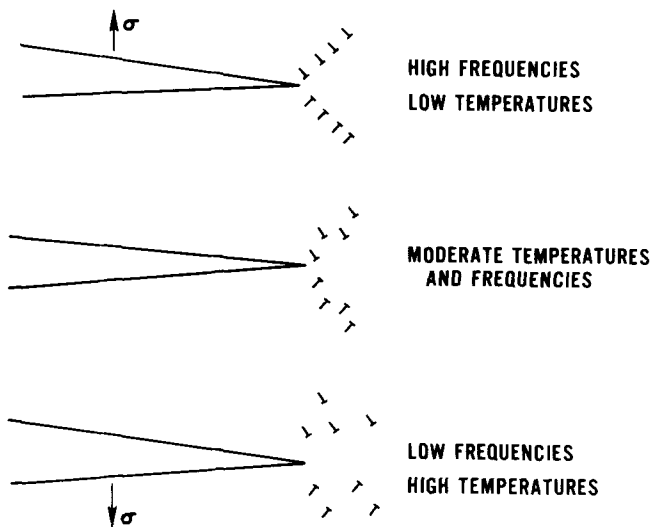


Fig. 6—Schematic representation of the dislocation arrangements at the tip of Stage II fatigue cracks for various temperatures and cyclic frequencies.

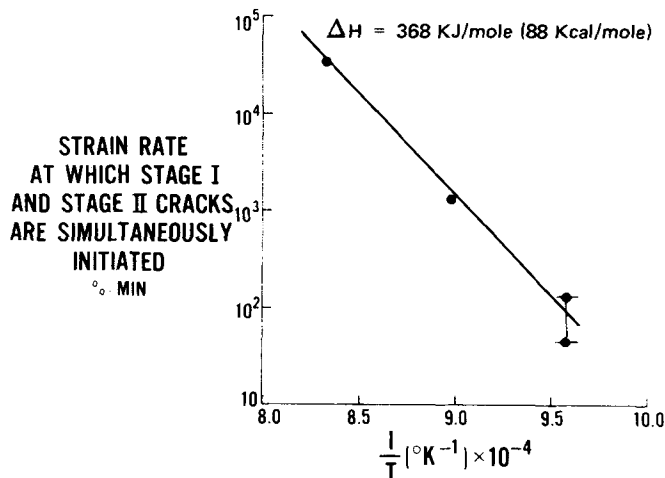


Fig. 7—Strain rate (cyclic frequency) at which Stage I and Stage II fatigue cracks are simultaneously initiated vs the inverse of the absolute temperature.

has been observed in other work.<sup>12-14</sup> Eventually, the fatigue lives reached a maximum level and then decreased at both 1033 and 1116 K. The decrease at highest frequencies is probably caused by an increase in intensity of the planar slip. Support for this argument comes from the fact that the fatigue lives at the highest frequencies at these two temperatures are the same as the room temperature lives,<sup>7</sup> and, for cycling at 10 Hz, at room temperature the concentration of dislocations in the planar bands is much greater than at 1033 K.<sup>1,2</sup>

The optimum lives occur under conditions of combined Stage II and Stage I crack initiation, where the dislocation density within the slip bands is relatively low and extensive creep is suppressed. This should lead to an increase in the frequency corresponding to the optimum cyclic life with increasing temperature. The data at 1200 K support this hypothesis, Fig. 1.

It is interesting to note that significant, reproducible variations in fatigue life were observed for tests in which crack initiation and most crack propagation occurred at subsurface locations, *i.e.*, in a virtual vacuum. Recent results for tantalum alloy Astar 811C,<sup>15</sup>

a copper-zirconium alloy,<sup>16</sup> cobalt-base alloy Mar-M302,<sup>17</sup> 304 stainless steel and iron-base alloy A-286<sup>18</sup> tested in vacuum or inert gas similarly show significant effects of cyclic frequency on low-cycle fatigue lives at elevated temperature.

The above studies confirm that a change in the level or intensity of cyclic plastic deformation by varying cyclic frequency can, by itself, affect elevated temperature fatigue lives. This is in contrast to situations where frequency affects fatigue lives through environmental interactions with the material.<sup>19,20</sup>

## CONCLUSIONS

1) At the lower temperatures and higher frequencies, cracks initiated and propagated in the Stage I mode (crystallographic cracking on the {111} slip planes). At the higher temperatures and lower frequencies, cracks initiated and propagated in the Stage II mode (perpendicular to the principal stress axis).

2) Stage I cracking occurred under conditions of heterogeneous, planar slip and Stage II cracking under conditions of homogeneous, wavy slip.

3) At a critical frequency at each temperature, Stage I and Stage II cracks were both initiated. The critical frequency was controlled by a thermally activated recovery process with an activation energy of 368 KJ/mole (88 Kcal/mole).

4) In contrast to classical low temperature fatigue behavior of most alloys, where Stage I cracking is followed by Stage II crack propagation, Stage II cracking often preceded Stage I crack propagation in the elevated temperature testing of this nickel-base superalloy.

5) An optimum frequency existed for maximizing fatigue life. Creep damage was detrimental at frequencies below the optimum and intense, planar slip at frequencies above the optimum. The optimum frequency increased with increasing temperature.

## REFERENCES

1. M. Gell and G. R. Leverant: *Fracture 1969*, p. 565, Chapman and Hall Ltd., London, 1969.
2. M. Gell, G. R. Leverant, and C. H. Wells: *Achievement of High Fatigue Resistance in Metals and Alloys*, pp. 113-53, ASTM STP 467, 1970.
3. G. R. Leverant and M. Gell: *Trans. TMS-AIME*, 1969, vol. 245, p. 1167.
4. G. R. Leverant, M. Gell, and S. W. Hopkins: *Proc. Second Int. Conf. on the Strength of Metals and Alloys*, p. 1141, ASM, vol. III, 1970.
5. G. R. Leverant, M. Gell, and S. W. Hopkins: *Mater. Sci. Eng.*, 1971, vol. 8, p. 125.
6. G. R. Leverant and B. H. Kear: *Met. Trans.*, 1970, vol. 1, p. 491.
7. D. J. Duquette and M. Gell: *Met. Trans.*, 1971, vol. 2, p. 1325.
8. F. E. Organ and M. Gell: *Met. Trans.*, 1971, vol. 2, p. 943.
9. D. J. Duquette and M. Gell: *Met. Trans.*, 1972, vol. 3, p. 1899.
10. J. P. Dennison, R. J. Llewellyn, and B. Wilshire: *J. Inst. Metals*, 1967, vol. 95, p. 115.
11. P. A. Flinn: *Trans. TMS-AIME*, 1960, vol. 218, p. 145.
12. G. P. Tilly: *Proc. Inst. Mech. Eng.*, 1965-66, vol. 180, p. 1045.
13. N. Stephenson: Memorandum No. M320, National Gas Turbine Establishment, Pyestock, Hants., England, June 1958.
14. J. E. Northwood, R. S. Smith, and N. Stephenson: Memorandum No. M325, National Gas Turbine Establishment, 1959.
15. K. D. Sheffler and G. S. Doble: *Influence of Creep Damage on the Low-Cycle Thermal-Mechanical Fatigue Behavior of Two Tantalum-Base Alloys*, NASA CR-121001, 1972.
16. J. B. Conway, R. H. Stenz, and J. T. Berling: *High Temperature, Low-Cycle Fatigue of Copper-Base Alloys in Argon: Part II*, NASA CR-121260, 1973.
17. K. D. Sheffler: TRW, Cleveland, Ohio, unpublished research.
18. K. D. Sheffler: *Vacuum Thermal-Mechanical Fatigue Testing of Two Iron-Base High Temperature Alloys*, NASA CR-134524.
19. L. F. Coffin, Jr.: *Met. Trans.*, 1972, vol. 3, p. 1777.
20. C. J. McMahon and L. F. Coffin, Jr.: *Met. Trans.*, 1970, vol. 1, p. 3443.